Human Hippocampal Theta Power Indicates Movement Onset and Distance Travelled

Daniel Bush[1,2,*,†], James A. Bisby[1,2,*], Chris M. Bird[3,*], Stephanie Gollwitzer[2,4], Roman Rodionov[2], Beate Diehl[2,5], Andrew W. McEvoy[2], Matthew C. Walker[2] and Neil Burgess[1,2†]

[1]UCL Institute of Cognitive Neuroscience, London, WC1N 3AZ, UK

[2]UCL Institute of Neurology, London, WC1N 3BG, UK

[3]School of Psychology, University of Sussex, Brighton, BN1 9QH, UK

[4]Department of Neurology, University Hospital Erlangen, D-91054, Erlangen, Germany

[5]Department of Clinical Neurophysiology, National Hospital for Neurology and Neurosurgery, London, WC1N 3BG, UK

*These authors contributed equally to this work

†Corresponding authors: drdanielbush@gmail.com, n.burgess@ucl.ac.uk

Running title: Movement Related Theta in Human Hippocampus

Classification: Biological Sciences, Neuroscience

Keywords: Theta, Hippocampus, Navigation, Spatial Memory, Intracranial EEG

Abstract

Theta frequency oscillations in the 6-10Hz range dominate the rodent hippocampal local field potential during translational movement, suggesting that theta encodes self-motion. Increases in theta power have also been identified in the human hippocampus during both real and virtual movement, but appear as transient bursts in distinct high and low frequency bands, and it is not yet clear how these relate to the sustained oscillation observed in rodents. Here, we examine depth electrode recordings from the temporal lobe of thirteen pre-surgical epilepsy patients performing a self-paced spatial memory task in a virtual environment. In contrast to previous studies, we focus on movement onset periods that incorporate both initial acceleration and an immediately preceding stationary interval associated with prominent theta oscillations in the rodent hippocampal formation. We demonstrate that movement onset periods are associated with a significant increase in both low (2-5Hz) and high (6-9Hz) frequency theta power in the human hippocampus. Similar increases in low and high theta power are seen across lateral temporal lobe recording sites, and persist throughout the remainder of movement in both regions. In addition, we show that movement related theta power is greater both prior to and during longer paths, directly implicating human hippocampal theta in the encoding of translational movement. These findings strengthen the connection between studies of theta band activity in rodents and humans and offer new insight into the neural mechanisms of spatial navigation.

Significance Statement

Rodent hippocampal theta band oscillations are observed throughout translational movement, implicating theta in the encoding of self-motion. Interestingly, increases in theta power are particularly prominent around movement onset. Here, we use intracranial recordings from epilepsy patients navigating in a desktop virtual reality environment to demonstrate that theta power is also increased in the human hippocampus around movement onset and throughout the remainder of movement. Importantly, these increases in theta power are greater both prior to and during longer paths, directly implicating human hippocampal theta in the encoding of translational movement. These findings help to reconcile previous studies of rodent and human hippocampal theta oscillations and provide new insight into the mechanisms of spatial navigation in the human brain.

\body

Introduction

The rodent hippocampal local field potential (LFP) is dominated by 6-10Hz theta oscillations during translational movement (1, 2). Both the power (1, 3) and frequency (3-6) of theta are positively correlated with running speed. Theta oscillations might therefore encode self-motion information and contribute to the generation of spatially modulated firing patterns (7-9). A critical concern for contemporary neuroscience is to establish whether this hypothesis can be translated across species. During navigation, intracranial recordings from depth electrodes in the human hippocampus have shown that theta is more prevalent during movement than stationary periods (10-12), and that theta power increases with movement speed (13). In addition, increases in movement related theta power are seen across the neocortex (10, 11, 14). These findings support the hypothesis that human theta oscillations might encode self-motion information. However, it has also been demonstrated that human theta band activity typically occurs in transient bursts distributed throughout movement, in contrast to the continuous high amplitude oscillation observed in the rodent (15, 16). Moreover, these studies identified movement related oscillations within both high theta and low theta / delta frequency bands (17-20). Hence, it is not yet clear how theta oscillations in the human hippocampus relate to those observed in the rodent.

To address this question, we examine intracranial recordings from the temporal lobe of pre-surgical epilepsy patients performing a self-paced spatial memory task (21). In contrast to previous studies, we focus on analysing changes in oscillatory power around movement onset in the virtual environment. In the rodent hippocampal formation, theta power increases are observed during the stationary period immediately prior to movement initiation in both the membrane potential oscillations of single neurons (22) and in the LFP (1, 2, 23-26). In addition, MEG recordings in healthy human participants have identified a transient increase in theta power around virtual movement onset that is correlated with subsequent spatial memory performance, although the source of this oscillation could not be localised (27). Here, we demonstrate that movement onset is associated with a significant increase in both low and high theta power across the human hippocampus and lateral temporal lobe that persists throughout the remainder of movement. Moreover, we find that increases in movement related theta power are greater for longer paths, directly implicating human hippocampal theta in the encoding of translational movement. These findings support the translation of hypotheses regarding movement related theta from rodent models, and provide new insights into the mechanisms of human spatial navigation.

Results

Behavioural Data. Nineteen pre-surgical epilepsy patients with depth electrodes implanted in the temporal lobe performed a spatial memory task in a virtual reality (VR) environment (21, 27, 28; Figure 1A). Temporal lobectomy patients have been shown to be impaired on a similar task (29), and performance on this task has been related to increases in hippocampal activity in previous fMRI studies (21, 27). Briefly, during encoding, patients were asked to navigate towards and memorise the location of four visible objects. During retrieval, patients were cued with an image of one object, then placed back in the environment and asked to navigate towards the remembered location of that (now

invisible) object and make a response. This provides a continuous measurement of distance error Δd between the location at which patients made a response and the true location of the object in each retrieval trial. The object then appeared in its correct location, to provide patients with feedback on their performance and allow further learning. The feedback period ended when patients navigated to the location of the now visible object.

Three patients did not complete the task due to technical difficulties, one patient could not perform the task, and two patients failed to produce sufficient stationary periods due to continuous movement. For the remaining thirteen patients (see Tables S1a, b for details), mean distance error was Δd = 28.7±14.4 virtual metres (vm; range of 10.5 – 49.6vm), which is smaller than chance performance (~49.4vm, t(12)=-5.19, p<0.001, Cohen's d=1.44; Figures 1B, C). In addition, there was a significant reduction in distance error for each object across retrieval trials (t(12)=-2.25, p<0.05, d=0.62; Figure 1D), suggesting that the feedback provided at the end of each trial led to an improvement in patient's performance. These results indicate that patients could successfully perform the task.

Increased Hippocampal Theta Power around Movement Onset. In the rodent hippocampal formation, significant increases in theta power have been observed during the stationary period immediately prior to movement onset (1, 2, 22-26). To establish whether similar increases in theta power could be observed in the human hippocampus, we focussed our analysis on a 1s period centred on movement onset that includes both the initial period of acceleration and an immediately preceding stationary interval (see Materials and Methods). We began by comparing low frequency oscillatory power on hippocampal electrode contacts during these movement onset periods with periods of complete immobility across encoding and retrieval phases (excluding all trials that contained interictal spike artefacts, see Table S2 for trial counts). The resultant power spectrum exhibits two peaks centred around ~3.5Hz and 7Hz, respectively (Figure 2A, B), consistent with previous human intracranial studies that have described distinct task-related changes in separate 'low' and 'high' theta bands (17-20). No significant ERPs were observed around movement onset, suggesting that these power increases reflect induced oscillations (Figure S1). In addition, a comparison of power spectra for the remainder of movement and stationary periods also revealed peaks in the low and high theta bands (Figure 2C; see Figure S2 for separate power spectra from each condition).

To further characterise these changes, we extracted mean z-scored power values from 3Hz windows around the observed peaks in the low and high theta band (i.e. 2-5Hz and 6-9Hz, respectively) for all movement periods. A repeated measures ANOVA with levels of frequency band (low v high theta), task phase (encoding v retrieval) and movement period (movement onset v remainder of movement v stationary) revealed a main effect of movement period on hippocampal theta power (F(2,16)=10.1, p=0.001, η_p^2=0.56), but no effect of frequency band or task phase and no interactions (all p>0.17; Figure 2D). Subsequent analyses indicated that this arose from an increase in theta power during movement onset compared to stationary periods (t(8)=4.78, p<0.005, d=1.59), consistent with previous rodent studies and our prior hypothesis (2, 26). We also note a trend towards greater theta power during movement onset compared to remainder of movement periods (t(8)=2.16, p=0.06, d=0.72); and during remainder of movement compared to stationary periods (t(8)=2.24, p=0.06, d=0.75), although neither of these contrasts reached statistical significance. Moreover, z-scored theta

power was greater than zero (i.e. from mean power in that frequency band across the entire recording, including task and non-task periods) during both movement onset ($t(8)=3.56$, $p<0.01$, $d=1.19$) and remainder of movement ($t(8)=2.51$, $p<0.05$, $d=0.84$), but not stationary ($t(8)=-0.33$, $p=0.75$, $d=0.11$), periods. Subsequent analysis indicated that these findings were not affected by differences in clinical criteria among the patient population (see Supplementary Information).

These results demonstrate that a large but transient increase in both low and high human hippocampal theta power accompanies the onset of movement in a virtual reality environment, analogous to the increase in rodent hippocampal theta power immediately prior to the onset of physical movement (1, 2, 22-26). Importantly, this effect may have been overlooked by previous paradigms that have compared 'pure' movement and stationary periods (10-12, 14). Although theta power is strongest around movement onset, however, it does not differ statistically from the remainder of movement ($p<0.06$) and remains elevated above baseline levels throughout both periods. Additional analyses indicate that theta power increases are specific to translational movements, as no analogous changes in low frequency power are observed during the onset or remainder of purely rotational movement (Figure S3). Interestingly, we also found no evidence for a difference in the magnitude of theta power increases around movement onset between encoding and retrieval periods. These findings are consistent with sensor level MEG recordings using a similar paradigm (27) and suggest that the hippocampus may be one source of that observed signal, although other potential sources cannot be ruled out.

Increased Theta Power in the Lateral Temporal Lobe around Movement Onset. Next, we asked whether movement related theta oscillations were restricted to hippocampal electrode contacts or also present in other temporal lobe regions. In rodents, theta has been observed in the amygdala during emotional arousal (30, 31); and in pre- and infra- limbic cortices during spatial memory tasks (32, 33). In humans, theta oscillations appear to be widespread across the neocortex during navigation in VR environments (10, 11, 14), as well as during short- and long- term memory tasks (28, 34, 35). We therefore analysed changes in z-scored theta power between movement periods across patients with depth electrode contacts located in the amygdala (n=12 patients) and lateral temporal lobe (n=12 patients; for complementary analysis of n=8 patients with electrode contacts in all three regions, see Supplementary Information).

For electrode contacts located in the amygdala, we note a trend towards a main effect of movement period ($F(2,22)=3.09$, $p=0.07$, $\eta_p^2=0.22$), but no other main effects or interactions (Figure 2E, see Table S3 for trial counts). In addition, mean z-scored power values across both task phases and frequency bands were not different from zero during any movement period (all $p>0.09$). Electrode contacts located in the lateral temporal lobe showed a main effect of movement period ($F(2,22)=3.77$, $p<0.05$, $\eta_p^2=0.26$), but no other main effects or interactions (all $p>0.19$; Figure 2F, Table S4 for trial counts). Subsequent analyses demonstrated that, as in the hippocampus, this arose from an increase in theta power during movement onset periods compared to stationary periods ($t(11)=2.35$, $p<0.05$, $d=0.68$), while there was no difference in theta power between movement onset periods and the remainder of movement ($t(11)=1.74$, $p=0.11$, $d=0.50$), or between remainder of movement and stationary periods ($t(11)=1.24$, $p=0.24$, $d=0.36$). Moreover, mean z-scored theta power was greater than zero during movement onset ($t(11)=2.48$, $p<0.05$, $d=0.72$), but not remainder of movement or stationary

periods (both p>0.27). Again, these findings were not affected by differences in clinical criteria among the patient population (see Supplementary Information).

These results demonstrate that changes in movement related theta power within the amygdala and lateral temporal lobe show the same general pattern as those in the hippocampus, although these differences only reach significance on lateral temporal lobe electrode contacts. In light of this, we asked whether theta oscillations recorded on medial and lateral electrode contacts were the product of independent sources or a single theta generator. To answer this question, we examined the phase offset between theta band oscillations on all pairs of electrode contacts in the hippocampus and lateral temporal lobe during movement onset periods. We found that the distribution of phase lags across patients was unimodal with zero mean in both the low (circular v=8.30, p<0.001) and high (circular v=8.89, p<0.001) theta band. Similarly, distributions of trial by trial phase lags across all electrode pairs in the low and high theta band for each individual patient were also unimodal with zero mean (all circular V>54.1, all p<0.001). Next, we examined the relationship between trial by trial variations in power within each region during movement onset periods. We found that trial by trial power in the hippocampus and lateral temporal lobe were highly correlated in both the low (t(8)=10.36, p<0.001, d=3.45) and high (t(8)=8.05, p<0.001, d=2.68) theta bands. Each of these results is consistent with the influence of a single theta generator on both regions. Further analyses indicated that theta oscillations recorded on lateral temporal lobe contacts were unlikely to arise as a result of volume conduction from the hippocampus (see Supplementary Information; 36). Hence, it appears that theta oscillations across the temporal lobe are actively driven by a single source. Although these data are insufficient to determine the location of that source, we note that that theta synchrony across the hippocampal formation in rodents is thought to be driven by common input from the medial septum (26).

Movement Related Theta Power is Greater during Longer Paths. Having established that movement onset and, to a lesser extent, remainder of movement periods were accompanied by a transient increase in theta power across the hippocampus and lateral temporal lobe, we asked whether theta amplitude during these periods had any behavioural correlates. Previous human intracranial EEG studies have demonstrated that theta power correlates with movement speed (13) and is greater when navigating more complex trajectories (15, 37). In our task, movement in the virtual environment accelerated quickly to a fixed top speed. However, we were able to examine whether theta power varied with distance travelled during each translational movement, by separating movement onset and remainder of movement periods for each patient according to whether the distance travelled was longer or shorter than their median path length.

In the hippocampus, a repeated measures ANOVA with levels of frequency band (low v high theta), movement period (movement onset v remainder of movement) and path length (long v short) showed a main effect of path length on theta power (F(1,8)=8.28, p<0.05, η_p^2=0.51), in addition to the expected main effect of movement period described above (F(1,8)=9.63, p<0.05, η_p^2=0.55), but no other main effects or interactions (all p>0.65). Subsequent analyses demonstrated that this resulted from higher theta power both prior to and during longer paths (t(8)=2.88, p<0.05, d=0.96; Figure 3A, B). Importantly, z-scored power was also greater than zero both prior to and during long (t(8)=4.12, p<0.005, d=1.37) but not short (t(8)=0.77, p=0.46, d=0.26) paths.

Data from lateral temporal lobe contacts revealed similar results: a significant main effect of path length ($F(1,11)=29.37$, $p<0.001$, $\eta_p^2=0.73$), but no other main effects or interactions (all $p>0.06$), which resulted from increased theta power prior to and during long, compared to short, paths ($t(11)=5.42$, $p<0.001$, $d=1.56$; Figures 3C, D); with z-scored theta power being greater than zero prior to and during long ($t(11)=4.32$, $p<0.005$, $d=1.18$) but not short ($t(11)=1.34$, $p=0.22$, $d=0.20$) paths (for complementary analysis of n=8 patients with electrode contacts in all regions, see Supplementary Information). In both cases, we note that changes in movement related oscillatory power between short and long paths were not restricted to the low and high theta band, but could be observed across a broad range of frequencies (<30Hz, see Figures 3B, D). While this may be partly accounted for by spectral leakage from peaks in the low and high theta band, the modulation of oscillatory power in other frequency bands might be addressed by future studies. Again, these results were generally unaffected by differences in clinical criteria among the patient population (see Supplementary Information). In addition, we found no evidence for differences in movement related theta power according to the duration of the stationary period preceding movement, where spatial orienting may occur; or between trials with high and low performance on electrode contacts in any region (see Supplementary Information, all $p>0.12$).

Hence, theta power increases across the temporal lobe during both movement onset and remainder of movement periods are most pronounced for longer paths across the virtual environment, but do not appear to co-vary with task performance. These results are consistent with movement related theta oscillations mediating spatial processing, rather than necessarily determining memory performance during encoding or retrieval: theta power being increased immediately prior to and throughout translational movements, while the magnitude of that power increase indicates distance travelled. Moreover, these findings implicate theta oscillations in spatial updating during both the planning and execution of translational movements (2).

Discussion

We have demonstrated that both low and high theta power in the human hippocampus and lateral temporal lobe are increased around movement onset in a virtual environment, compared to stationary periods. These theta power increases appear to peak during the stationary interval immediately prior to movement onset (Figure 2B), although our movement onset periods also incorporate an initial period of acceleration that may contribute to the observed effect. Analogous results have been obtained from the rodent hippocampus, where theta power increases are seen immediately prior to the onset of translational movement in both the local field potential (1, 2, 23-26) and in the membrane potential of single neurons (22). Hence, this finding strengthens the translational connection between studies of movement related theta in human and rodent models. Importantly, this increase in theta power around movement onset may have been overlooked by previous human intracranial recording studies that have exclusively compared 'pure' movement and stationary periods that tend to be of short duration (10-12, 14). Theta power increases are not specific to movement onset periods, however: both low and high theta power remained above baseline levels during the remainder of movement in the hippocampus and, to a lesser extent, in the lateral temporal lobe. These data are consistent with the rodent literature and several previous intracranial studies that have

described an increased prevalence of theta band oscillations during movement compared to stationary periods in both the hippocampus and neocortex (10-12).

In addition, we have shown that movement related increases in both theta bands are greater both prior to and during longer paths, while neither appears to correlate significantly with task performance or vary in power between periods of encoding and retrieval. These results suggest a role for theta oscillations in both the planning and execution of translational movements during an ethologically valid navigation task. This is consistent with several previous studies showing that theta oscillations are more prevalent during complex spatial navigation tasks (i.e. long versus short mazes; 15, 37), faster translational movements (13), and virtual teleportation over longer versus shorter distances in the absence of visual or self-motion cues (38). Importantly, this study also extends those results by focussing on changes in theta power, which can be more easily related to rodent data than the prevalence of theta oscillations; by examining active self-directed movements, which have greater ethological validity than periods of passive movement or teleportation; and by showing increased theta power prior to the onset of longer paths, supporting the hypothesis that theta oscillations are involved in spatial updating during the planning, as well as the execution, of translational movements (2).

Previous studies have highlighted two important differences between rodent and human movement related theta oscillations (20). First, human theta oscillations appear in transient bursts that typically last several cycles, in contrast to the continuous rhythm in the rodent hippocampus (15, 16), which casts doubts on whether these sporadic oscillations could encode continuous self-motion information (8, 20). However, it is possible that location estimates are updated intermittently during theta bursts, in accordance with the outcome of planned movements, rather than tracked continually throughout movement by an ongoing theta oscillation. Such a mechanism would be consistent with our observation that theta power was greater prior to movement onset and for longer translational movements. Alternatively, estimates of current location might be intermittently updated by tracking the relative location of visual landmarks during theta bursts; and distance travelled might be estimated by tracking the temporal duration of each translational movement. Further investigation using experimental paradigms that can dissociate the relative influence of temporal duration and visual input on estimates of distance travelled are required to address this issue (38).

Second, human movement related theta oscillations apparently exist in two different frequency bands – one lower, and closer to the traditional delta band; and one higher, and closer to the frequency of rodent hippocampal theta (10, 13, 20). It has been suggested that low theta may be the analogue of rodent hippocampal theta as it shows more prominent subsequent memory effects (17, 18); phase coupling with rhinal cortices (39); and modulates the firing rate of hippocampal cells during virtual navigation (40). Two distinct hippocampal theta oscillations have also been identified in rodents: Type 1, which is typically modulated by translational movement and has a higher frequency; and Type 2, which is typically modulated by anxiety and arousal and has a lower frequency, though still clearly above the delta band (41). However, the fact that both low and high theta power appear to be modulated by translational movement in our data, while no manipulations of anxiety or arousal were made, suggests that both correspond to rodent Type 1 theta. In fact, we found no evidence for a functional distinction between low and high theta oscillations during any movement period, suggesting that these frequency bands might coexist to mediate human spatial processing. It is also possible that low and high theta do not reflect independent processes, but a single oscillation that

varies dynamically over a broad frequency range (42, 43). This could explain the presence of spike-LFP phase coupling in single neurons within the human hippocampal formation in the absence of a strong fixed frequency baseline oscillation (40). Interestingly, the zero phase lag observed here between theta oscillations on hippocampal and lateral temporal lobe electrode contacts contrasts with previous reports of stable non-zero phase differences between theta oscillations in these regions during a non-spatial memory task (19). This might be accounted for by mnemonic function preferentially recruiting Type 2 theta oscillations that are independently generated by separate hippocampal and cortical sources.

Three important caveats to the results presented here merit further discussion. First, contrasts between movement and stationary periods are confounded by the fact that patients must press a button to move across the virtual reality environment but not to remain stationary. This raises the possibility that observed changes in theta power result from button pressing, rather than translational movement per se. However, our data shows that button pressing in the absence of translational movement is not associated with changes in either low or high theta power (see Figure S4 and accompanying text), consistent with several previous studies showing no correlation between button pressing and theta power in the human hippocampus or neocortex (10, 11, 34, 36). Second, it is important to emphasise that patients do not physically locomote during the task. In rodents, both movement related theta oscillations and the spatial modulation of neural firing patterns are weaker during passive movement through an environment (44, 45). Similarly, although LFP theta oscillations appear normal in rodent VR recordings (22, 46), the relationship between running speed and theta frequency is reduced (47). Hence, it is possible that the power, duration and spectral fingerprint of movement related theta in humans may differ during physical locomotion. Interestingly, recent depth electrode recordings taken from the hippocampi of a small number of patients hint at an increased prevalence of high frequency theta oscillations during real world ambulation (12). Finally, all human intracranial EEG studies must address the issue of extrapolating findings in epilepsy patients to the wider population. Reassuringly, the results presented here qualitatively replicate findings from a previous MEG study of healthy participants performing a similar task (27). The increase in theta power around movement onset observed in that study could not be localised, but the data presented here suggest the hippocampus as one candidate– although other potential sources cannot be ruled out. Further investigation with more advanced MEG source localisation techniques might elucidate this issue (48).

In summary, we have shown that movement onset is associated with a pronounced increase in both low and high theta power in the human hippocampus that also persists during the remainder of movement. Importantly, movement related theta power is also greater both prior to and during longer translational paths. These findings strengthen the link between rodent and human hippocampal theta oscillations and provide new insights into the mechanisms of human spatial navigation.

Materials and Methods

Nineteen patients with pharmaco-resistant epilepsy completed a spatial memory task used in several previous neuroimaging studies (21, 27, 28; Figure 1A) in which they are asked to remember object locations in the absence of direct cues, similar to the Morris water maze (49). Of those, three were excluded due to technical difficulties, one patient could not perform the task, and two patients failed to produce a sufficient number of stationary trials as they moved continuously in the VR environment. This left thirteen patients: six female and eleven right-handed, with a mean age ± SD of 29.3 ± 7.8 years (see Tables S1a, b for further details). Four patients completed one session of the task, and nine patients completed two sessions. The second session made use of the same environment but used four new objects in new locations.

Surgery and subsequent intracranial recordings were carried out at the National Hospital for Neurology and Neurosurgery, London. All patients had platinum Spencer probe depth electrodes (Severn Healthcare Technologies, Newbury, Berkshire, UK) inserted into the medial temporal lobe: eight patients in the right hemisphere, four in the left hemisphere and one bilateral implantation. Electrode locations were determined solely by clinical criteria, ascertained by visual inspection of post-implantation CT and / or MRI scans by a trained neurologist (RR), and verified by an fMRI expert (JAB). The presence of hippocampal damage was assessed, when histopathology was not available, by structural MRI at 3T including quantification of hippocampal volumes and T2 relaxation times. The study was approved by the NHS ethics committee, and all patients gave written informed consent. Patients were seizure free for at least 24 hours before participation.

Depth EEG was recorded continuously at a sample rate of 1024Hz (patients 4 and 10) or 512Hz (all other patients) using either a Nicolet NicOne long-term monitoring system (Natus Neurology, Middleton WI, USA; patients 1-6) or Micromed SD long-term monitoring system (Micromed, Mogliano Veneto, Treviso, Italy; patients 7-13). Recordings made at a higher sampling rate were down-sampled to 512Hz, to match those from the majority of patients, before any analyses were performed. Recordings made using the Micromed system were also subject to a 0.02Hz digital high-pass filter. For each patient, a post-implantation CT image showing the implanted electrodes was co-registered with, and then overlaid upon, a pre-implantation T1-weighted MR image. Candidate reference electrodes were chosen from contacts located in white matter by visual inspection of the overlaid images. EEG recordings from each candidate reference electrode were then visually inspected, and a single contact with little or no apparent EEG activity chosen as the reference for all subsequent recordings. Audio triggers produced by the VR laptop were recorded on the monitoring system, allowing EEG to be aligned with movement and task information sampled at 25Hz.

Further information can be found in the SI Materials and Methods.

Acknowledgements

The authors would like to thank all patients that participated in this study, as well as Mike Anderson, Helen Barron, Aidan Horner, Raphael Kaplan, Catherine Scott and Ewa Zotow for useful discussions during the preparation of this manuscript. This work was supported by the Wellcome Trust, MRC, and the Department of Health's NIHR UCLH/UCL Biomedical Research Centre.

References

[1] Vanderwolf CH (1969) Hippocampal electrical activity and voluntary movement in the rat. EEG Clinical Neurophysiology 26: 407 – 418

[2] O'Keefe J, Nadel L (1978) The Hippocampus as a Cognitive Map. Oxford University Press, Oxford, UK

[3] McFarland WL, Teitelbaum H, Hedges EK (1975) Relationship between hippocampal theta activity and running speed in the rat. Journal of Comparative and Physiological Psychology 88(1): 324-328

[4] Rivas J, Gaztelu JM, García-Austt E (1996) Changes in hippocampal cell discharge patterns and theta rhythm spectral properties as a function of walking velocity in the guinea pig. Experimental Brain Research 108: 113-118

[5] Sławińska U, Kasicki S (1998) The frequency of rat's hippocampal theta rhythm is related to the speed of locomotion. Brain Research 796: 327-331

[6] Jeewajee A, Barry C, O'Keefe J, Burgess N (2008) Grid cells and theta as oscillatory interference: electrophysiological data from freely-moving rats. Hippocampus 18: 1175 – 1185

[7] Brandon MP, Bogaard AR, Libby CP, Connerney MA, Gupta K, Hasselmo ME (2011) Reduction of theta rhythm dissociates grid cell spatial periodicity from directional tuning. Science 332: 595–599

[8] Burgess N, O'Keefe J (2011) Models of place and grid cell firing and theta rhythmicity. Current Opinion in Neurobiology 21: 734-744

[9] Koenig J, Linder AN, Leutgeb JK, Leutgeb S (2011) The spatial periodicity of grid cells is not sustained during reduced theta oscillations. Science 332: 592–595

[10] Ekstrom AD, Caplan JB, Ho E, Shattuck K, Fried I, Kahana MJ (2005) Human hippocampal theta activity during virtual navigation. Hippocampus 15(7): 881-889

[11] Jacobs J, Korolev IO, Caplan JB, Ekstrom AD, Litt B, Baltuch G, Fried I, Schulze-Bonhage A, Madsen JR, Kahana MJ (2009) Right-lateralized Brain Oscillations in Human Spatial Navigation. Journal of Cognitive Neuroscience 22(5): 824-836

[12] Bohbot VD, Copara MS, Gotman J, Ekstrom AD (2017) Low-frequency theta oscillations in the human hippocampus during real-world and virtual navigation. Nature Communications 8: 14415

[13] Watrous AJ, Fried I, Ekstrom AD (2011) Behavioral correlates of human hippocampal delta and theta oscillations during navigation. Journal of Neurophysiology 105(4): 1747-1755

[14] Caplan JB, Madsen JR, Schulze-Bonhage A, Aschenbrenner-Scheibe R, Newman EL, Kahana MJ (2003) Human theta oscillations related to sensorimotor integration and spatial learning. Journal of Neuroscience 23(11): 4726-4736

[15] Kahana MJ, Sekuler R, Caplan JB, Kirschen M, Madsen JR (1999) Human theta oscillations exhibit task dependence during virtual maze navigation. Nature 399(6738): 781-784

[16] Watrous AJ, Lee DJ, Izadi A, Gurkoff GG, Shahlaie K, Ekstrom AD (2013) A comparative study of human and rat hippocampal low-frequency oscillations during spatial navigation. Hippocampus 23(8): 656-661

[17] Sederberg PB, Schulze-Bonhage A, Madsen JR, Bromfield EB, McCarthy DC, Brandt A, Tully MS, Kahana MJ (2007) Hippocampal and neocortical gamma oscillations predict memory formation in humans. Cerebral Cortex 17(5): 1190-1196

[18] Fell J, Ludowig E, Staresina BP, Wagner T, Kranz T, Elger CE, Axmacher N (2011) Medial temporal theta/alpha power enhancement precedes successful memory encoding: evidence based on intracranial EEG. Journal of Neuroscience 31(14): 5392-5397

[19] Lega BC, Jacobs J, Kahana MJ (2011) Human hippocampal theta oscillations and the formation of episodic memories. Hippocampus 22(4): 748-761

[20] Jacobs J (2014) Hippocampal theta oscillations are slower in humans than in rodents: implications for models of spatial navigation and memory. Philosophical Transactions of the Royal Society London B: Biological Sciences 369(1635): 20130304

[21] Doeller CF, King JA, Burgess N (2008) Parallel striatal and hippocampal systems for landmarks and boundaries in spatial memory. PNAS 105(15): 5915-5920

[22] Schmidt-Hieber C, Häusser M (2013) Cellular mechanisms of spatial navigation in the medial entorhinal cortex. Nature Neuroscience 16: 325-31

[23] Green JD, Arduini AA (1954) Hippocampal electrical activity in arousal. Journal of Neurophysiology 17(6): 533-557

[24] Whishaw IQ, Vanderwolf CH (1973) Hippocampal EEG and behavior: changes in amplitude and frequency of RSA (theta rhythm) associated with spontaneous and learned movement patterns in rats and cats. Behavioural Biology 8(4): 461-484

[25] Bland BH, Jackson J, Derrie-Gillespie D, Azad T, Rickhi A, Abriam J (2006) Amplitude, Frequency, and Phase Analysis of Hippocampal Theta During Sensorimotor Processing in a Jump Avoidance Task. Hippocampus 16: 673-681

[26] Fuhrmann F, Justus D, Sosulina L, Kaneko H, Beutel T, Friedrichs D, Schoch S, Schwarz MK, Fuhrmann M, Remy S (2015) Locomotion, Theta Oscillations, and the Speed-Correlated Firing of Hippocampal Neurons Are Controlled by a Medial Septal Glutamatergic Circuit. Neuron 86(5): 1253-1264

[27] Kaplan R, Doeller CF, Barnes GR, Litvak V, Düzel E, Bandettini PA, Burgess N (2012) Movement-related theta rhythm in humans: coordinating self-directed hippocampal learning. PLoS Biology 10(2): e1001267

[28] Kaplan R, Bush D, Bonnefond M, Bandettini PA, Barnes GR, Doeller CF, Burgess N (2014) Medial prefrontal theta phase coupling during spatial memory retrieval. Hippocampus 24(6): 656-665

[29] Spiers HJ, Burgess N, Maguire EA, Baxendale SA, Hartley T, Thompson PJ, O'Keefe J (2001) Unilateral temporal lobectomy patients show lateralised topographical and episodic memory deficits in a virtual town. Brain 124: 2476-2489

[30] Seidenbecher T, Laxmi TR, Stork O, Pape HC (2003) Amygdalar and hippocampal theta rhythm synchronization during fear memory retrieval. Science 301(5634): 846-850

[31] Paré D, Collins DR, Pelletier JG (2002) Amygdala oscillations and the consolidation of emotional memories. Trends in Cognitive Science 6(7): 306-314

[32] Young CK, McNaughton N (2009) Coupling of theta oscillations between anterior and posterior midline cortex and with the hippocampus in freely behaving rats. Cerebral Cortex 19(1): 24-40

[33] Benchenane K, Peyrache A, Khamassi M, Tierney PL, Gioanni Y, Battaglia FP, Wiener SI (2010) Coherent theta oscillations and reorganization of spike timing in the hippocampal- prefrontal network upon learning. Neuron 66(6): 921-936

[34] Raghavachari S, Kahana MJ, Rizzuto DS, Caplan JB, Kirschen MP, Bourgeois B, Madsen JR, Lisman JE (2001) Gating of human theta oscillations by a working memory task. Journal of Neuroscience 21(9): 3175-3183

[35] Sederberg PB, Kahana MJ, Howard MW, Donner EJ, Madsen JR (2003) Theta and gamma oscillations during encoding predict subsequent recall. Journal of Neuroscience 23(34): 10809-10814

[36] Sirota A, Montgomery S, Fujisawa S, Isomura Y, Zugaro M, Buzsaki G (2008) Entrainment of Neocortical Neurons and Gamma Oscillations by the Hippocampal Theta Rhythm. Neuron 60: 683-697

[37] Caplan JB, Madsen JR, Raghavachari S, Kahana MJ (2001) Distinct patterns of brain oscillations underlie two basic parameters of human maze learning. Journal of Neurophysiology 86(1): 368-380

[38] Vass LK, Copara MS, Seyal M, Shahlaie K, Farias ST, Shen PY, Ekstrom AD (2016) Oscillations Go the Distance: Low-Frequency Human Hippocampal Oscillations Code Spatial Distance in the Absence of Sensory Cues during Teleportation. Neuron 89: 1180-1186

[39] Fell J, Klaver P, Elfadil H, Schaller C, Elger CE, Fernández G (2003) Rhinal-hippocampal theta coherence during declarative memory formation: interaction with gamma synchronization? European Journal of Neuroscience 17(5): 1082-1088

[40] Jacobs J, Kahana MJ, Ekstrom AD, Fried I (2007) Brain oscillations control timing of single-neuron activity in humans. Journal of Neuroscience 27(14): 3839-3844

[41] Kramis R, Vanderwolf CH, Bland BH (1975) Two types of hippocampal rhythmical slow activity in both the rabbit and the rat: Relations to behavior and effects of atropine, diethyl ether, urethane, and pentobarbital. Experimental Neurology 49: 58-85

[42] Cohen MX (2014) Fluctuations in oscillation frequency control spike timing and coordinate neural networks. Journal of Neuroscience 34(27): 8988-8998

[43] Orchard J (2015) Oscillator-interference models of path integration do not require theta oscillations. Neural Computation 27(3): 548-560

[44] Terrazas A, Krause M, Lipa P, Gothard KM, Barnes CA, McNaughton BL (2005) Self-motion and the hippocampal spatial metric. Journal of Neuroscience 25(35): 8085-8096

[45] Winter SS, Mehlman ML, Clark BJ, Taube JS (2015) Passive Transport Disrupts Grid Signals in the Parahippocampal Cortex. Current Biology 25(19): 2493-2502

[46] Harvey CD, Collman F, Dombeck DA, Tank DW (2009) Intracellular dynamics of hippocampal place cells during virtual navigation. Nature 461(7266): 941-946

[47] Ravassard P, Kees A, Willers B, Ho D, Aharoni D, Cushman J, Aghajan ZM, Mehta MR (2013) Multisensory control of hippocampal spatiotemporal selectivity. Science 340(6138): 1342-1346

[48] Meyer SS, Rossiter H, Brookes MJ, Woolrich MW, Bestmann S, Barnes GR (2017) Using generative models to make probabilistic statements about hippocampal engagement in MEG. Neuroimage 149: 468-482

[49] Morris RGM, Garrud P, Rawlins JNP, O'Keefe J (1982) Place navigation impaired in rats with hippocampal lesions. Nature 297: 681-683

[50] Lachaux J-P, Rodriguez E, Martinerie J, Varela FJ (1999) Measuring phase synchrony in brain signals. Human Brain Mapping 8: 194-208

[51] Berens P (2009) CircStat: A Matlab Toolbox for Circular Statistics. Journal of Statistical Software 31(10)

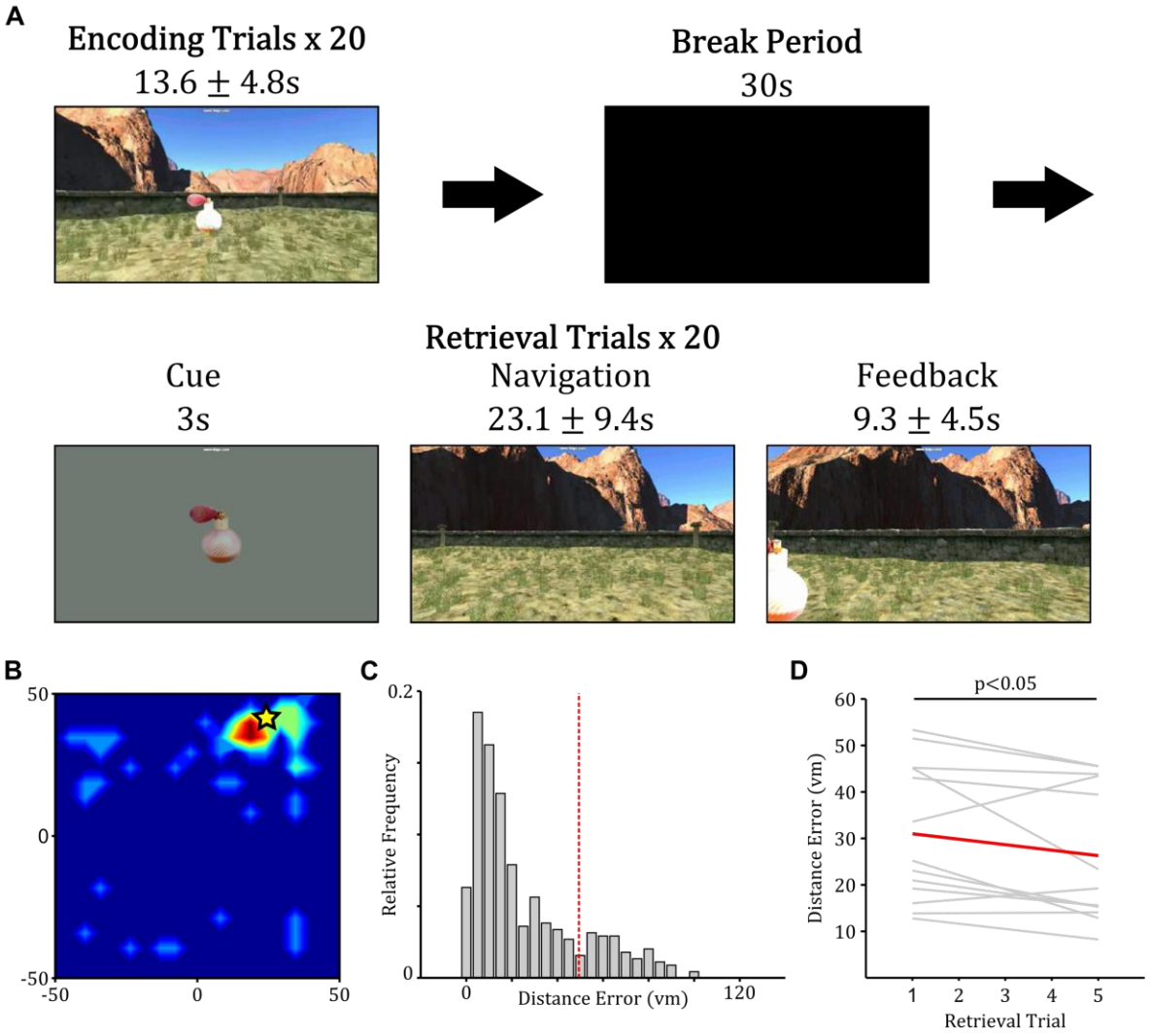
A
Encoding Trials x 20
13.6 ± 4.8s
Break Period
30s
Retrieval Trials x 20
Cue
3s
Navigation
23.1 ± 9.4s
Feedback
9.3 ± 4.5s
B
50
0
-50
-50
0
50
C
0.2
0
Relative Frequency
0
Distance Error (vm)
120
D
p<0.05
60
50
40
30
20
10
Distance Error (vm)
1
2
3
4
5
Retrieval Trial

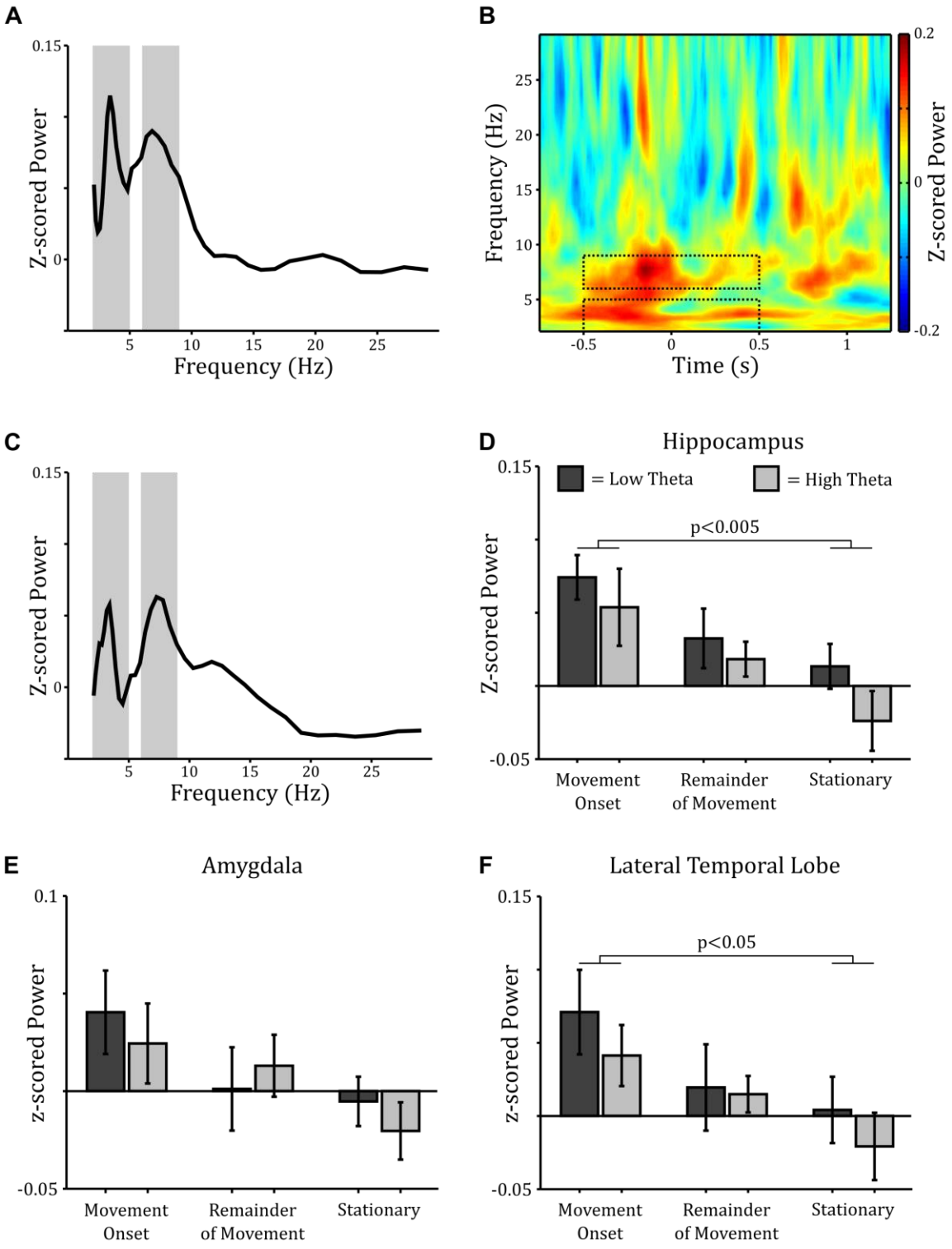
A
0.15
Z-scored Power
0
5
10
15
20
25
Frequency (Hz)
B
Frequency (Hz)
25
20
15
10
5
-0.5
0
0.5
1
Time (s)
0.2
0
-0.2
Z-scored Power
C
0.15
Z-scored Power
0
5
10
15
20
25
Frequency (Hz)
D
Hippocampus
= Low Theta
= High Theta
p<0.005
0.15
Z-scored Power
-0.05
Movement Onset
Remainder of Movement
Stationary
E
Amygdala
0.1
z-scored Power
-0.05
Movement Onset
Remainder of Movement
Stationary
F
Lateral Temporal Lobe
p<0.05
0.15
z-scored Power
-0.05
Movement Onset
Remainder of Movement
Stationary

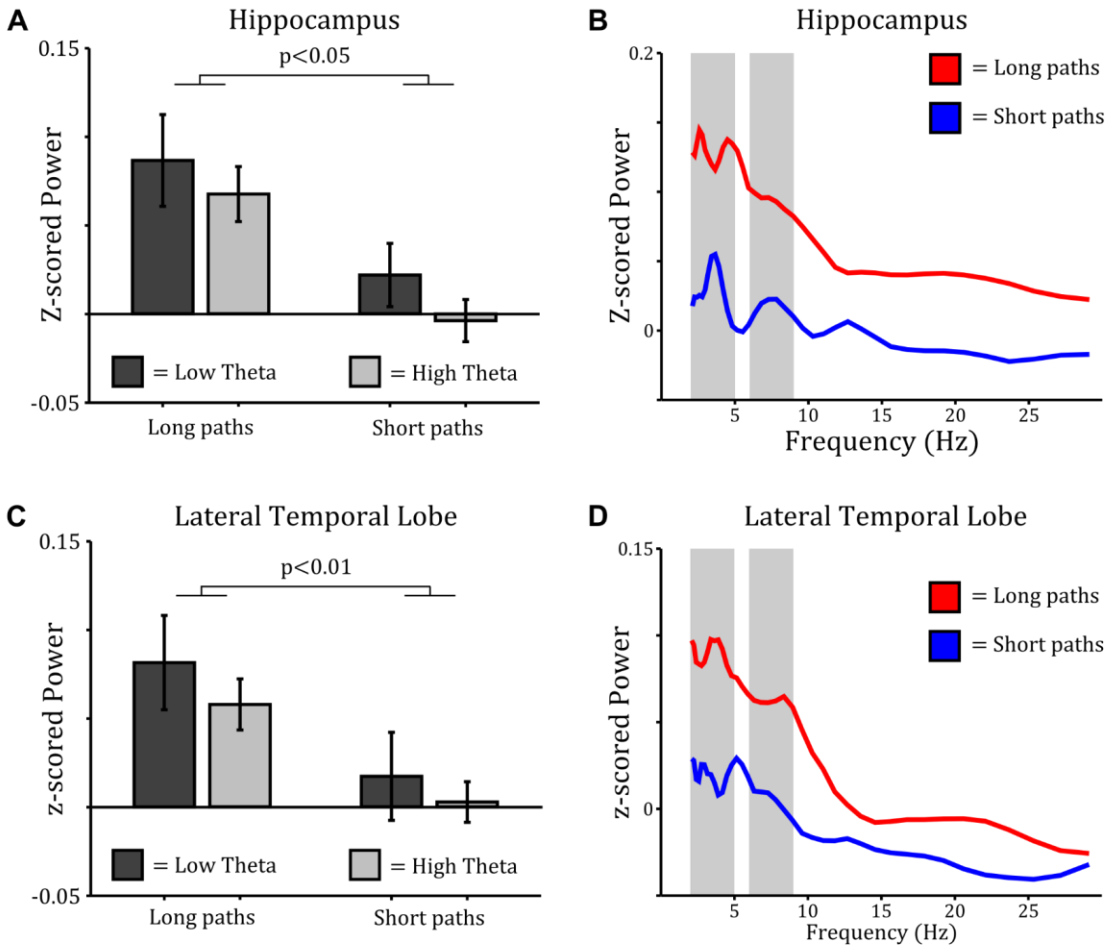
A
Hippocampus
p<0.05
0.15
-0.05
Z-scored Power
= Low Theta
= High Theta
Long paths
Short paths
B
Hippocampus
0.2
0
Z-scored Power
= Long paths
= Short paths
5
10
15
20
25
Frequency (Hz)
C
Lateral Temporal Lobe
p<0.01
0.15
-0.05
z-scored Power
= Low Theta
= High Theta
Long paths
Short paths
D
Lateral Temporal Lobe
0.15
0
z-scored Power
= Long paths
= Short paths
5
10
15
20
25
Frequency (Hz)

Figure Legends

Figure 1: Behavioural Data. **(A)** Schematic of the spatial memory task. Participants navigate freely in a 100m sided square VR environment with distal cues for orientation. Participants memorise the location of one of four objects across twenty encoding trials (five for each object). Encoding is followed by a 30s break period during which participants are instructed to focus on memorising object locations. Each of twenty retrieval trials (five for each object) begins with a 3s cue period, during which an image of one object is presented on screen. Participants are then placed back at one of four starting locations and instructed to navigate to the remembered location of that object and make a response. Following this response, the object appears in its correct location to provide feedback on their performance in each trial. **(B)** Heat map of all responses for the object location in session one with the largest mean error across patients. True object location is marked with a yellow star. **(C)** Histogram of distance errors across all objects and patients. Chance performance is marked with a red dashed line. **(D)** Change in mean distance error for all objects across retrieval trials. Linear fits to each patient's performance are marked with a light grey line, and the average marked with a thick red line.

Figure 2: Theta Power changes during Virtual Movement across the Temporal Lobe. **(A)** Average power spectrum for movement onset periods, baseline corrected by mean power at each frequency during stationary periods, for electrode contacts in the hippocampus. Power is increased in both low (2-5Hz) and high (6-9Hz) theta bands (marked in grey). **(B)** Spectrogram of power around virtual movement onset, baseline corrected by mean power at each frequency during stationary periods, for electrode contacts in the hippocampus. Black dashed regions indicate the low and high theta bands for the 1s period around movement onset. **(C)** Average power spectrum for remainder of movement periods, baseline corrected by mean power at each frequency during stationary periods, for electrode contacts in the hippocampus. Peaks in the low and high theta bands (marked in grey) are visible, but less pronounced than during movement onset. **(D, E, F)** Mean z-scored power in the low (2-5Hz) and high (6-9Hz) theta bands during movement onset, remainder of movement and stationary periods in the (D) hippocampus; (E) amygdala; and (F) lateral temporal lobe. Both low and high theta power are significantly increased during virtual movement onset, compared to stationary periods, on electrode contacts in the hippocampus and lateral temporal lobe, but not those located in the amygdala. In addition, mean z-scored power in the low and high theta bands are greater than zero during movement onset on electrode contacts in the hippocampus and lateral temporal lobe; and during the remainder of movement on electrode contacts in the hippocampus.

Figure 3: Theta Power changes with Path Length in the Hippocampus and Lateral Temporal Lobe. **(A, C)** Mean z-scored power in the low (2-5Hz) and high (6-9Hz) theta bands averaged across movement onset and remainder of movement periods for long and short paths across the virtual environment on (A) hippocampal and (C) lateral temporal lobe electrode contacts. In each region, both low and high theta power are significantly increased during long, compared to short, paths. **(B, D)** Power spectra averaged across movement onset and remainder of movement periods for long and short paths across the virtual environment in the (B) hippocampus and (D) lateral temporal lobe. In both regions, broadband low frequency oscillatory power is increased during long, compared to short, paths. Low (2-5Hz) and high (6-9Hz) theta bands are marked in grey.

Supplementary Information

Materials and Methods

Patient population

Nineteen patients with pharmaco-resistant epilepsy were recruited. Of those, three were excluded due to technical difficulties, one patient could not perform the task, and two patients failed to produce a sufficient number of stationary trials as they moved continuously in the VR environment. This left thirteen patients: six female and eleven right-handed, with a mean age ± SD of 29.3 ± 7.8 years (see Tables S1a, b for further details). Surgery and subsequent intracranial recordings were carried out at the National Hospital for Neurology and Neurosurgery, London. All patients had platinum Spencer probe depth electrodes (Severn Healthcare Technologies, Newbury, Berkshire, UK) inserted into the medial temporal lobe: eight patients in the right hemisphere, four in the left hemisphere and one bilateral implantation. Electrode locations were determined solely by clinical criteria, ascertained by visual inspection of post-implantation CT and / or MRI scans by a trained neurologist (RR), and verified by an fMRI expert (JAB). The presence of hippocampal damage was assessed, when histopathology was not available, by structural MRI at 3T including quantification of hippocampal volumes and T2 relaxation times. The study was approved by the NHS ethics committee, and all patients gave written informed consent. Patients were seizure free for at least 24 hours before participation.

Task

Patients completed a spatial memory task used in several previous neuroimaging studies (21, 27, 28; Figure 1A) in which they are asked to remember object locations in the absence of direct cues, similar to the Morris water maze (49). Participants navigate freely in a 100 virtual metre sided square virtual reality (VR) environment, which is projected onto a laptop screen placed in front of them. Movement within the VR environment is controlled using arrow keys on the laptop keyboard, with virtual movement accelerating quickly to a fixed top speed. Distal cues surround the environment to orient the participant.

During each encoding trial, participants are asked to navigate towards and encode the location of one of four different objects. Only one object is visible in each encoding trial, and there are five encoding trials for each of the four objects (giving a total of twenty encoding trials in each session). Object locations are constant across encoding trials. Following encoding, participants are given a 30s break during which they are instructed to focus on memorising the object locations. After the break period, each retrieval trial begins with a 3s cue period during which an image of one object is displayed on a plain grey background. Participants are subsequently placed back in the virtual environment at a randomly selected one of four starting locations and orientations, and asked to navigate to the remembered location of that object and make a response. Once participants have made a response, the object appears in its correct location to provide feedback on their performance, and the trial ends when participants navigate to the true location of the visible object. There are five retrieval trials for each object, giving a total of twenty retrieval trials in each session.

Four patients completed one session of the task, and nine patients completed two sessions. The second session made use of the same environment but used four new objects in new locations. The

distance error *Δd* for each trial is defined as the absolute distance between the location at which the response was made and the true location of that object. Chance performance was calculated as the mean distance between the location of each object and every other location in the environment (i.e. by treating every location in the environment as an equally likely response location). Changes in distance error across retrieval trials were assessed by first performing linear regression on the distance error in each trial against the retrieval trial number for that object, averaging those regression coefficients across objects for each patient, and performing a one-sampled t-test on mean regression coefficients across patients.

iEEG Recordings and Artefact Detection

Depth EEG was recorded continuously at a sample rate of 1024Hz (patients 4 and 10) or 512Hz (all other patients) using either a Nicolet NicOne long-term monitoring system (Natus Neurology, Middleton WI, USA; patients 1-6) or Micromed SD long-term monitoring system (Micromed, Mogliano Veneto, Treviso, Italy; patients 7-13). Recordings made at a higher sampling rate were down-sampled to 512Hz, to match those from the majority of patients, before any analyses were performed. Recordings made using the Micromed system were also subject to a 0.02Hz digital high-pass filter. For each patient, a post-implantation CT image showing the implanted electrodes was co-registered with, and then overlaid upon, a pre-implantation T1-weighted MR image. Candidate reference electrodes were chosen from contacts located in white matter by visual inspection of the overlaid images. EEG recordings from each candidate reference electrode were then visually inspected, and a single contact with little or no apparent EEG activity chosen as the reference for all subsequent recordings.

Audio triggers produced by the VR laptop were recorded on the monitoring system, allowing EEG to be aligned with movement and task information sampled at 25Hz. We analyse recordings from electrode contacts in three regions of interest: the hippocampus (nine patients with mean ± SD of 4.8 ± 1.6 contacts, range 2 – 8 contacts), amygdala (twelve patients with 2.7 ± 0.7 contacts, range 2 – 4 contacts) and lateral temporal lobe (twelve patients with 7.3 ± 3.0 contacts, range 2 – 12 contacts; see Table S1a for further details). These recordings, which included all experimental sessions performed by each patient as well as several minutes of EEG from before and after those sessions, were first inspected for interictal spike (IIS) events and other artefacts by a trained epileptologist (SG) and verified independently by an EEG analysis expert (DB). The timing of all IIS and other artefacts on each channel were recorded and stored for subsequent analyses. All analyses were carried out using custom Matlab (Mathworks, Natick, USA) scripts.

Epochs of Interest

Analysis of EEG recordings focussed on three main periods of interest: movement onset, remainder of movement, and stationary periods. Movement onset epochs were defined as -0.5:0.5s windows around the onset of periods of continuous translational movement in the virtual environment that lasted >1s and were preceded by periods of complete immobility (i.e. an absence of either translational or rotational movement) that lasted >0.5s. This was motivated by three factors: that the time window be centred on movement onset, to incorporate both the initial period of acceleration

and an immediately preceding stationary period associated with prominent theta power increases in the rodent hippocampus (1, 2, 22-26); that the window be of sufficient duration to assay changes in low frequency power (i.e. ≥1s, to incorporate ≥2 cycles of an oscillation at ≥2Hz); and that the time window be short enough to provide a sufficient number of remainder of movement trials of at least the same duration (i.e. ≤1s, given that the average movement duration across patients was ~2s, see Tables S2-S4).

Remainder of movement epochs were defined as >1s time windows of continuous translational movement within the virtual environment that lasted >1.5s, beginning 0.5s after the onset of movement and ending when movement ceased. Stationary epochs were defined as >1s time windows of complete immobility within the virtual environment that lasted >1.5s, beginning immediately after the cessation of movement and ending 0.5s before the onset of subsequent movement (see Tables S2-4 for trial counts and movement epoch lengths for all patients).

Event-related Potential Analysis

Event-related potentials (ERPs) for each epoch of interest were obtained by extracting raw EEG signals for each trial, subtracting the mean amplitude across that trial, and then z-scoring using the mean and standard deviation of signal amplitude across the entire recording on each channel. EEG signals from all artefact free trials during the same epoch were then averaged to generate the ERP for that epoch. To identify any significant ERPs, we performed one-sample t-tests at each time point with a more stringent threshold of $p<0.001$ to compensate for multiple comparisons across n=1024 time points. Significant ERPs were subsequently defined as any set of at least 25 contiguous time points (i.e. ≥50ms period) that exceeded this threshold.

Time-Frequency Analysis

Estimates of dynamic oscillatory power during periods of interest were obtained by convolving the EEG signal with a five cycle Morlet wavelet and squaring the absolute value of the convolved signal. The wavelet transform was preferred to the Fourier transform as it does not assume stationarity in EEG recordings. Power values were obtained for thirty-nine logarithmically spaced frequency bands in the 2-30Hz range. Time frequency data were extracted from 1s prior to the start of, to 1s after the end of, each period of interest, and data from those 1s epochs discarded after convolution to avoid edge effects. All trials that included IIS or other artefacts – either within the period of interest or the 1s padding windows - were excluded from all analyses presented here (see Tables S2-4 for trial counts). All power values were log transformed, and power values from each electrode for each condition were then z-scored using the mean and standard deviation of log-transformed power values in each frequency band during artefact free periods throughout the entire EEG recording.

To generate power spectra, the mean of dynamic oscillatory power estimates or differences in oscillatory power between conditions was taken over the time window of interest. To perform baseline correction on time-frequency data for display purposes (i.e. Figures 2A, B, C), log-transformed power values were averaged across stationary periods for each frequency band, and those average values subtracted from the log-transformed power values at each time point in the movement onset

or remainder of movement data. To examine changes in oscillatory power within specific frequency bands and assess correlations between oscillatory power, task performance and IIS events in each trial, dynamic estimates of log-transformed oscillatory power were averaged over the time and frequency windows of interest. Mean power values were then averaged across all electrode contacts in each cortical region to provide a single value for each patient. Changes in oscillatory power according to task demands were analysed using repeated measures ANOVAs and post-hoc one-sample t-tests with Bonferroni correction for multiple comparisons where appropriate.

Phase Coupling Analysis

To estimate the phase offset between simultaneous theta band oscillations on pairs of electrode contacts, the signal from each region – including a 1s window both before the start and after the end of each epoch – was band pass filtered in the frequency range of interest (i.e. 2-5Hz or 6-9Hz) using a zero phase, 400th order FIR filter. The phase difference between all pairs of electrode contacts between regions at each time point was then extracted. Phase coupling was estimated using the phase locking value, which is equal to the resultant vector length of the phase difference distribution across the time window of interest (50). Finally, the circular mean phase difference between filtered signals from each pair of electrode contacts within each epoch was computed, and then the circular mean value across all pairs of electrode contacts from each patient entered into a second level circular V test using the Toolbox for Circular Statistics in Matlab (51), in order to assess whether the distribution of phase differences across patients was drawn from a unimodal distribution with zero mean.

Results

Event Related Potentials at Virtual Movement Onset

It is important to ascertain whether the observed increase in theta power around the onset of movement in the virtual reality environment results from induced or evoked oscillations. In the latter case, one might expect to observe a simultaneous event related potential (ERP). Hence, we examined EEG from each cortical region at movement onset for any evidence of ERPs. However, we found no significant time-locked deflections in EEG recordings from either the hippocampus (Figure S1A, B), amygdala (Figure S1C, D) or lateral temporal lobe (Figure S1E, F) that might explain the observed increase in theta power shown in Figure 2. Hence, we conclude that these power changes reflect induced, rather than evoked, oscillations.

Raw Power Spectra for each Movement Condition across Temporal Lobe Recording Sites

In order to ascertain whether peaks were present in the low and high theta band during each movement condition separately, or whether such peaks were specific to movement onset and remainder of movement periods, separate power spectra from each cortical region were generated for each movement condition (Figure S2). These power spectra demonstrate that peaks in both the low and high theta band can be observed during movement onset periods in all cortical regions, alongside a general increase in low frequency (<10Hz) oscillatory power above baseline levels (i.e. above the mean power in that frequency band across the whole recording). Conversely, during stationary periods, peaks are observed in the low theta band only, and low frequency power is generally reduced compared to baseline levels.

Differences in Movement Related Theta Power according to Clinical Criteria

Given that the EEG recordings examined here are taken from a clinical population, we wished to assess whether any of the main effects observed – that is, increased theta power during movement onset, compared to stationary periods; and increased theta power both prior to and during longer translational paths – were influenced by clinical criteria. Between-subjects factors that might affect these results include the implanted hemisphere (language dominant v non-dominant), presence of hippocampal sclerosis, and presence of a temporal lobe seizure onset zone (see Table S1b for further details). Hence, we compared the magnitude of theta power changes between groups of patients that differed according to these criteria using a series of independent samples t-tests. In each case, we must note that the relatively small sample sizes used urge some caution when interpreting these findings.

First, we found no differences in the magnitude of theta power increases during movement onset, compared to stationary periods, on hippocampal electrode contacts between patients with depth electrodes implanted in the language dominant versus non-dominant hemisphere; with or without hippocampal sclerosis; and with or without a temporal seizure onset zone (all $p>0.1$). Similarly, we found no differences in theta power increases during movement onset, compared to stationary periods, on either amygdala or lateral temporal lobe electrode contacts between patients with depth

electrodes implanted in the language dominant v non-dominant hemisphere; with or without hippocampal sclerosis; and with or without a temporal seizure onset zone (all p>0.28).

Second, we found no evidence for differences in theta power during long versus short paths between patients with or without sclerotic hippocampi, and with or without a temporal seizure onset zone in any region (all p>0.21). Interestingly, however, the observed theta power increases for long versus short paths did show a trend towards laterality on hippocampal electrode contacts, being greater in patients with electrodes implanted in the language dominant hemisphere (t(7)=2.25, p=0.06, Cohen's d=0.80). Conversely, no such laterality was observed in either the amygdala or lateral temporal lobe (both p>0.13).

Theta Power Changes Associated with Rotational Movement

In order to ascertain whether changes in theta power were specific to translational movement, we analysed changes in low and high theta power during equivalent periods of purely rotational movement: 1s 'rotation onset' epochs centred on the onset of purely rotational movements that lasted >1s and were preceded by periods of complete immobility that lasted >0.5s; and >1s 'remainder of rotation' epochs beginning 0.5s after the onset of continuous rotational movement within the virtual environment that lasted >1.5s and ending when that movement ceased.

For electrode contacts in the hippocampus, a repeated measures ANOVA with levels of theta band (low v high) and rotation epoch (rotation onset v remainder of rotation v stationary) showed no main effects or interactions (all p>0.16; Figure S3A-D). However, we note a trend towards z-scored low theta power during rotation onset periods being greater than zero (i.e. from the mean power in that frequency band across the entire recording; t(8)=2.29, p=0.052, d=0.76, all other p>0.13). Similar results were obtained from electrode contacts in the amygdala, where no main effects or interactions were identified (all p>0.12) and z-scored power was not greater than zero in any condition (all p>0.15, Figure S3E); and in the lateral temporal lobe, where no main effects or interactions were identified (all p>0.14), although we note a similar trend towards z-scored low theta power during rotation onset periods being greater than zero (t(8)=2.20, p=0.05, d=0.64; all other p>0.38, Figure S3F). Overall, these results suggest that movement related changes in theta power are specific to translational movements, as purely rotational movements do not significantly modulate theta power in any temporal lobe region.

Comparison of Theta Power Changes across Temporal Lobe Recording Sites

To ascertain whether we could identify any systematic differences in z-scored theta power across temporal lobe recording sites during movement, we analysed data from eight patients who had depth electrode contacts in all three cortical regions. A repeated measures ANOVA with levels of theta band (low v high), region (hippocampus v amygdala v lateral temporal lobe) and movement epoch (movement onset v remainder of movement v stationary) revealed a main effect of movement epoch (F(2,14)=11.58, p=0.001, η_p^2=0.62), but no other main effects or interactions (all p>0.34). Subsequent analyses demonstrated that this results from an increase in theta power during movement onset, compared to both the remainder of movement (t(7)=3.02, p<0.05, d=1.07) and stationary periods

(t(7)=5.47, p<0.001, d=1.93). Moreover, z-scored theta power was greater than zero during movement onset periods (t(7)=4.79, p<0.005, d=1.70), but during neither remainder of movement nor stationary periods (both p>0.17).

Similarly, we characterised changes in theta power with path length across temporal lobe recording sites by analysing data from the same eight patients. In addition to the expected main effect of movement (F(1,7)=18.57, p<0.005, η_p^2=0.73), a repeated measures ANOVA with levels of theta band (low v high), cortical region (hippocampus v amygdala v lateral temporal lobe), movement epoch (movement onset v remainder of movement) and path length (long v short) identified a main effect of path length (F(1,7)=5.81, p<0.05, η_p^2=0.45) and a region x path length interaction (F(1,7)=8.76, p<0.005, η_p^2=0.56; all other p>0.09). Subsequent analyses demonstrate that these effects were driven by increased theta power during longer paths (t(7)=2.41, p<0.05, d=0.85); and a difference in theta power between the lateral temporal lobe and amygdala during long paths (t(7)=3.33, p<0.05, d=1.18; with no difference between the hippocampus and amygdala or lateral temporal lobe, both p>0.1). Hence, data from recordings across the temporal lobe in these eight patients generally show the same pattern of results described for hippocampal and lateral temporal lobe electrode contacts in the main text, with theta power elevated during movement onset; and movement related theta power being greater for longer translational paths.

Theta Oscillations in Lateral Temporal Lobe do not Reflect Volume Conduction from Hippocampus

Given that theta oscillations recorded on electrode contacts in the hippocampus and lateral temporal lobe during movement onset exhibited unimodal phase lag distributions with zero mean and had highly correlated trial by trial values across patients, we asked whether theta oscillations in the lateral temporal lobe might reflect volume conduction from the hippocampus. Volume conduction is commonly associated with three additional characteristics: a reduction in oscillatory power with distance from the anatomical source; an increase in phase offset, relative to the anatomical source, with distance from that source; and a decrease in the magnitude of phase coupling, relative to the anatomical source, with distance from that source (36). Hence, we examined low and high theta oscillations recorded simultaneously on electrode contacts in the hippocampus and lateral temporal lobe for each of these characteristics.

First, we found no significant relationship between the anatomical distance of lateral temporal lobe electrode contacts from the hippocampus and absolute theta power – that is, theta power in the lateral temporal lobe did not decrease with distance from hippocampal contacts in either the low (t(8)=-1.33, p=0.22) or high (t(8)=-0.97, p=0.36) theta band, although we do note a negative trend in each case. Second, we found no consistent relationship between the anatomical distance of lateral temporal lobe electrode contacts from the hippocampus and phase offset relative to hippocampal oscillations in either the low (t(8)=0.82, p=0.44, d=0.27) or high (t(8)=-1.32, p=0.22, d=0.44) theta band. Finally, we found that the magnitude of phase coupling with hippocampal electrode contacts did significantly decrease with anatomical distance from the hippocampus in both the low (t(8)=-3.12, p<0.05, d=1.04) and high (t(8)=-3.85, p<0.005, d=1.28) theta bands. In spite of this latter result, the overall pattern of findings described here do not support the hypothesis that theta oscillations on lateral temporal lobe contacts arise as a result of volume conduction from the hippocampus. Instead,

these findings are more consistent with the active entrainment of both regions by a single theta generator, although the location of that source cannot be determined from these data.

Theta Power Changes Associated with Spatial Orienting

In addition to examining changes in movement related theta power according to the length of translational paths (Figure 3), we also wished to ascertain whether theta power in either movement onset or remainder of movement epochs was affected by the duration of the preceding stationary period, when participants may have been orienting themselves within the environment. Hence, we split movement onset and remainder of movement epochs according to whether the duration of the immediately preceding stationary period was shorter or longer than the median duration across all trials for that patient.

For electrode contacts in the hippocampus, a repeated measures ANOVA with levels of theta band (low v high), movement epoch (movement onset v remainder of movement) and duration of preceding stationary period (short v long) revealed the expected main effect of movement epoch on theta power ($F(1,8)=7.97$, $p<0.05$, $\eta_p^2=0.50$), but no other main effects or interactions (all $p>0.16$). Similarly, for electrode contacts in both the amygdala and lateral temporal lobe, this analysis revealed no significant main effects or interactions (all $p>0.12$) although we do note a trend towards a main effect of movement epoch in the lateral temporal lobe ($F(1,11)=4.24$, $p=0.064$, $\eta_p^2=0.28$). Hence, these results suggest that the duration of stationary periods immediately prior to movement onset, during which spatial orienting may occur, has no effect on the magnitude of theta power increases observed either during movement onset or remainder of movement epochs.

Correlations between Theta Power and Performance

To analyse whether changes in theta power during movement onset and the remainder of movement covaried with task performance, we first split movement trials according to whether the mean distance error for the object being encoded or retrieved during that trial was above or below the median distance error across all objects during that session. For hippocampal electrode contacts, aside from the expected main effect of movement, a repeated measures ANOVA with levels of frequency band (low v high theta), movement epoch (movement onset v remainder of movement) and performance (good v bad) revealed no main effect of performance on theta power ($F(8,1)=2.66$, $p=0.14$, $\eta_p^2=0.25$) or interactions (all $p>0.55$). Similarly, for lateral temporal lobe electrode contacts, this analysis revealed no main effect of performance on theta power ($F(11,1)=0.64$, $p=0.44$, $\eta_p^2=0.06$) or interactions (all $p>0.31$). Second, we split movement trials during the retrieval period according to whether performance on that trial was above or below the median trial by trial distance error for that session, but a repeated measures ANOVA again revealed no effect of performance on theta power in the hippocampus ($F(8,1)=0.24$, $p=0.64$, $\eta_p^2=0.03$) and no interactions (all $p>0.51$). Similarly, for lateral temporal lobe electrode contacts, this analysis revealed no effect of performance on theta power ($F(11,1)=1.99$, $p=0.19$, $\eta_p^2=0.15$) and no interactions (all $p>0.08$). These findings suggest that movement related theta power increases are not predictive of spatial memory performance on this task.

Theta Power Changes Associated with Button Pressing

There is a possibility that the analyses of movement related changes in oscillatory power presented in the main text were confounded by button pressing, as patients must hold a button to move across the virtual environment, but not to remain stationary (see Materials and Methods). To address this issue, we analysed EEG data from response periods during retrieval trials in the spatial memory task when a button was pressed to indicate remembered object locations. Importantly, these response periods most often occurred during stationary periods, allowing us to disambiguate the oscillatory correlates of button pressing and translational movement. Hence, we analysed mean z-scored power in the low and high theta band during a -0.5:0.5s window around each response button press, excluding any trials where participants were moving during that 1s period (in addition to any trials containing IIS or other artefacts).

For electrode contacts in the hippocampus (mean ± SD = 23.7 ± 10.7 trials per patient), mean z-scored power during response periods was not different from zero in either the low ($t(8)=1.31$, $p=0.23$, $d=0.44$) or high ($t(8)=-0.62$, $p=0.55$, $d=0.21$) theta band (Figure S4A, B). Similarly, for electrode contacts in the amygdala (21.8 ± 11.0 trials per patient) and lateral temporal lobe (27.1 ± 11.0 trials per patient; Figure S4C), we identified no significant changes in low or high theta power during response periods (all $p>0.54$; Figure S4D). Hence, we conclude that the changes in movement related theta power shown in Figure 2 cannot be attributed to button pressing.

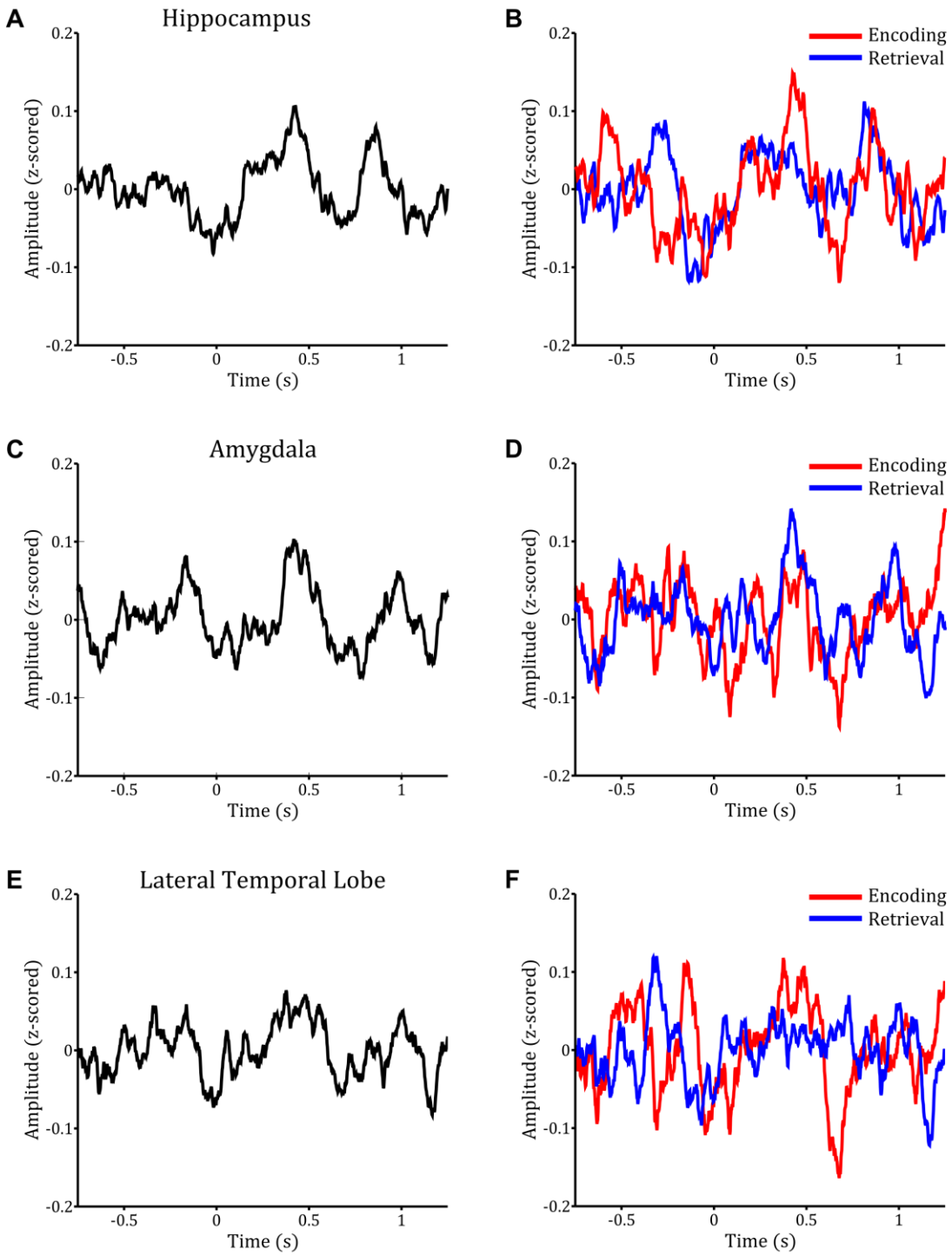
A
Hippocampus
Amplitude (z-scored)
Time (s)
B
Encoding
Retrieval
Amplitude (z-scored)
Time (s)
C
Amygdala
Amplitude (z-scored)
Time (s)
D
Encoding
Retrieval
Amplitude (z-scored)
Time (s)
E
Lateral Temporal Lobe
Amplitude (z-scored)
Time (s)
F
Encoding
Retrieval
Amplitude (z-scored)
Time (s)

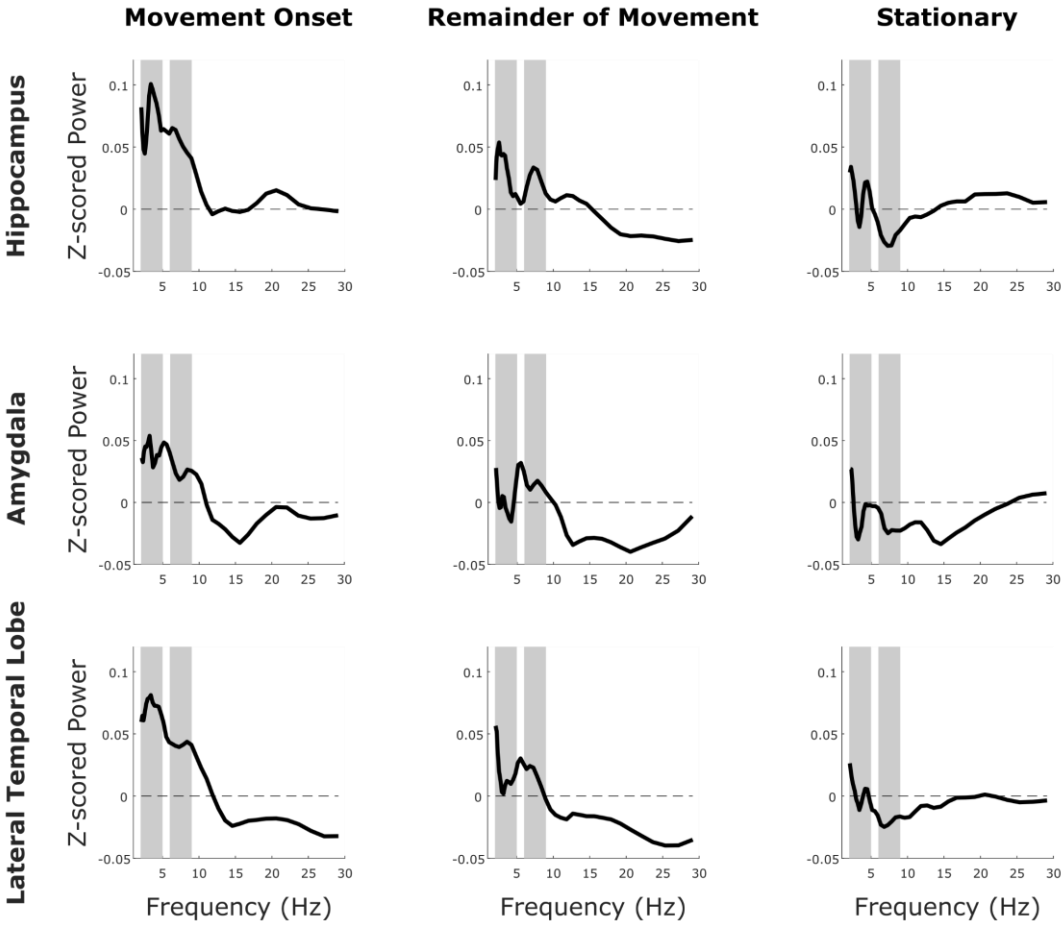
Movement Onset
Remainder of Movement
Stationary
Hippocampus
Amygdala
Lateral Temporal Lobe
Z-scored Power
0.1
0.05
0
-0.05
5
10
15
20
25
30
Frequency (Hz)

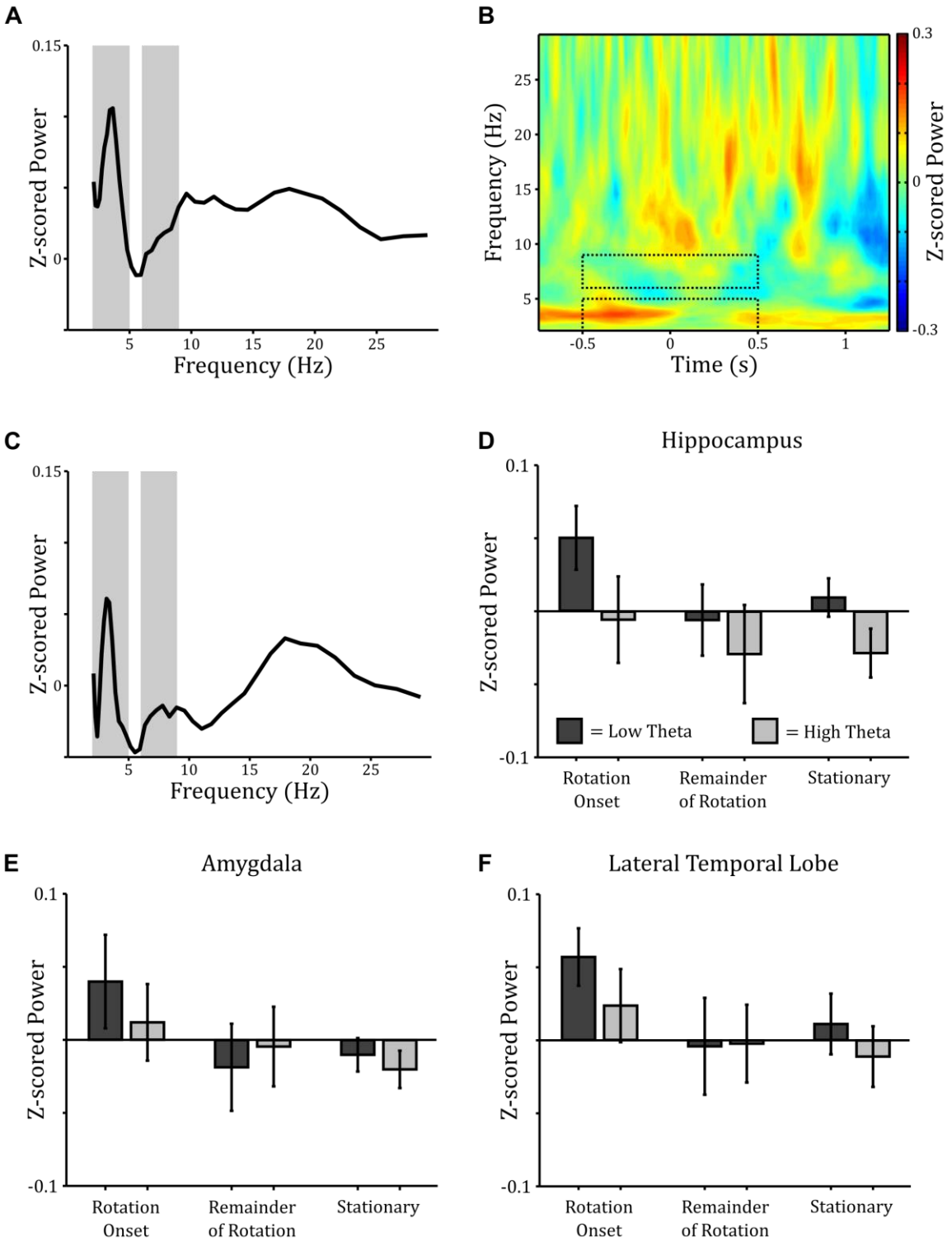
A
0.15
Z-scored Power
0
5
10
15
20
25
Frequency (Hz)
B
Frequency (Hz)
25
20
15
10
5
-0.5
0
0.5
1
Time (s)
0.3
0
-0.3
Z-scored Power
C
0.15
Z-scored Power
0
5
10
15
20
25
Frequency (Hz)
D
Hippocampus
0.1
-0.1
Z-scored Power
= Low Theta
= High Theta
Rotation Onset
Remainder of Rotation
Stationary
E
Amygdala
0.1
-0.1
Z-scored Power
Rotation Onset
Remainder of Rotation
Stationary
F
Lateral Temporal Lobe
0.1
-0.1
Z-scored Power
Rotation Onset
Remainder of Rotation
Stationary

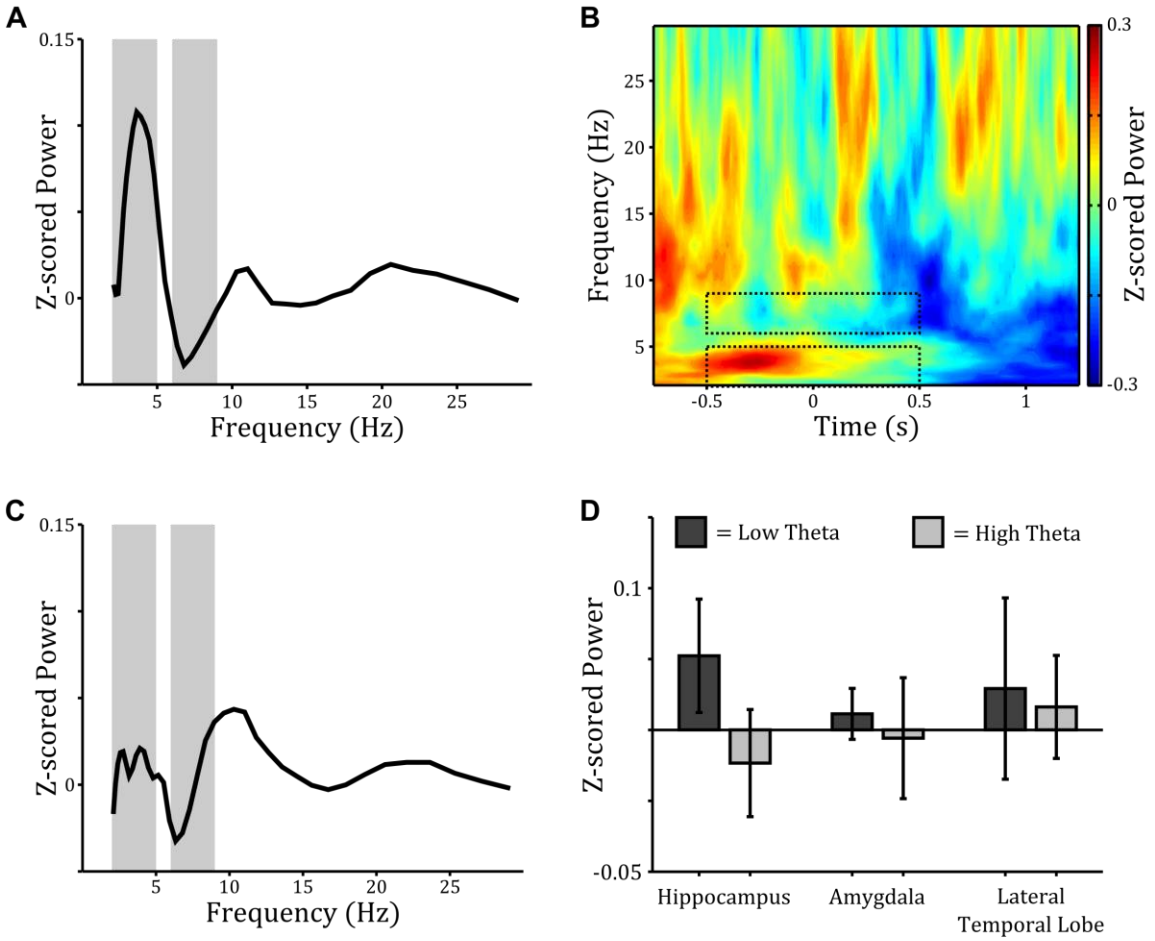
A
0.15
0
Z-scored Power
5
10
15
20
25
Frequency (Hz)
B
Frequency (Hz)
25
20
15
10
5
-0.5
0
0.5
1
Time (s)
0.3
0
-0.3
Z-scored Power
C
0.15
0
Z-scored Power
5
10
15
20
25
Frequency (Hz)
D
= Low Theta
= High Theta
0.1
-0.05
Z-scored Power
Hippocampus
Amygdala
Lateral
Temporal Lobe

Figure Legends

Supplementary Figure 1: Event related potentials (ERPs) at virtual movement onset averaged across all movement onset trials (left column) and separated by encoding and retrieval phases (right column) in the **(A, B)** hippocampus; **(C, D)** amygdala and **(E, F)** lateral temporal lobe

Supplementary Figure 2: Individual power spectra for electrode contacts in each cortical region and each movement condition, with low (2-5Hz) and high (6-9Hz) theta bands highlighted with light grey bars. Peaks in both the low and high theta bands are generally visible across movement onset conditions, while peaks in the low theta band only are visible during stationary periods. In addition, low frequency (<10Hz) power is generally greater during movement onset than both remainder of movement and stationary periods.

Supplementary Figure 3: Theta Power changes during Rotational Movement across the Temporal Lobe. **(A)** Average power spectrum for rotation onset epochs (mean ± SD = 53.3 ± 38.3 trials per patient), baseline corrected by mean power at each frequency during stationary periods (89.5 ± 76.2 trials per patient lasting 2.33 ± 0.51s), for electrode contacts in the hippocampus. Low (2-5Hz) and high (6-9Hz) theta bands are marked in grey. **(B)** Spectrogram of power around rotation onset, baseline corrected by mean power at each frequency during stationary periods, for electrode contacts in the hippocampus. Black dashed regions indicate the low and high theta bands for the 1s period around movement onset. **(C)** Average power spectrum for remainder of movement epochs (36.6 ± 26.1 trials per patient lasting 2.0 ± 0.16s), baseline corrected by mean power at each frequency during stationary periods, for electrode contacts in the hippocampus. Peaks in the low and high theta bands (marked in grey) are visible, but less pronounced than during movement onset. **(D, E, F)** Mean z-scored power in the low (2-5Hz) and high (6-9Hz) theta bands during rotation onset, remainder of rotation and stationary epochs in the (D) hippocampus; (E) amygdala (61.3 ± 29.0 rotation onset trials, 39.0 ± 19.5 remainder of rotation trials lasting 2.2 ± 0.3s, and 97.8 ± 60.3 stationary trials lasting 2.55 ± 0.55s per patient); and (F) lateral temporal lobe (62.6 ± 33.2 rotation onset trials, 40.9 ± 22.0 remainder of rotation trials lasting 2.18 ± 0.25s, and 102.0 ± 66.2 stationary trials lasting 2.46 ± 0.52s per patient). There are no significant changes in either low or high theta power across any of these epochs in any cortical region (all $p>0.08$).

Supplementary Figure 4: Theta Power Changes during Button Pressing. **(A)** Spectrum of mean z-scored power versus frequency on hippocampal electrodes during 1s response periods, which correspond to button pressing in the absence of translational movement. Low (2-5Hz) and high (6-9Hz) theta bands are marked in grey. **(B)** Spectrogram of z-scored power on hippocampal electrodes around button pressing in the absence of translational movement. Black dashed regions indicate the low and high theta bands for the 1s response period. **(C)** Spectrum of mean z-scored power versus frequency on lateral temporal lobe electrodes during 1s response periods, which correspond to button pressing in the absence of translational movement. Low (2-5Hz) and high (6-9Hz) theta bands are marked in grey. **(D)** Comparison of mean z-scored power in the low (dark grey) and high (light grey) theta band on electrode contacts in the hippocampus, amygdala and lateral temporal lobe during a 1s period around button pressing. There are no significant changes in either high or low theta power in any region.